

# The Effect of the Medium Polarity on the Mechanism of the Reaction of Hydroxybenzenes with Hydrazyl Radical in Aprotic Solvents

N. I. Belaya<sup>a\*</sup>, A. V. Belyj<sup>a</sup>, O. M. Zarechnaya<sup>b</sup>, I. N. Scherbakov<sup>c</sup>,  
V. M. Mikhailchuk<sup>a</sup>, and V. S. Doroshkevich<sup>a</sup>

<sup>a</sup> Donetsk National University, ul. Universitetskaya 24, Donetsk, 83001 Ukraine

\*e-mail: nat.iv.belaya@gmail.com

<sup>b</sup> Litvinenko Institute of Physico-Organic Chemistry and Coal Chemistry, Donetsk, Ukraine

<sup>c</sup> Southern Federal University, Rostov-on-Don, Russia

Received November 3, 2016

**Abstract**—Mechanisms of the reaction of di- and trihydroxybenzenes with 2,2'-diphenyl-1-picrylhydrazyl (stable radical) in aprotic media of different polarity have been elucidated by experimental and quantum-chemical methods. Kinetic, stoichiometric, and activation parameters of the reaction have been determined. In benzene (nonpolar solvent), the studied reaction occurs via the hydrogen atom transfer mechanism; in the polar solvent with weak ionizing ability (i.e. DMSO), the reaction predominantly occurs via the faster mechanism of coupled electron and proton transfer.

**Keywords:** hydroxybenzene, 2,2'-diphenyl-1-picrylhydrazyl, antiradical activity, reaction mechanism

**DOI:** 10.1134/S1070363217040053

Many methods are known to evaluate the anti-radical activity of natural phenolic compounds in view of application as antioxidants [1] using stable radicals, the most widely used being 2,2'-diphenyl-1-picrylhydrazyl (DPPH).

A special feature of the reaction of phenol with DPPH (Scheme 1) is strong influence of the solvent nature on the process kinetics.

In nonpolar media, the reaction slowly occurs via the cleavage of phenolic proton via the Hydrogen Atom Transfer (HAT) mechanism or as a coupled transfer of electron and proton (Proton-Coupled Electron Transfer, PCET) [2].

In polar solvents, the interaction of phenolic compounds with DPPH is a sequential transfer of electron and proton (Electron Transfer–Proton Transfer, ET–PT) or the same transfers in the reverse order

(Proton Transfer–Electron Transfer, PT–ET), depending on the ionizing ability of the medium [3–5].

Elucidation of the mechanism of phenol interaction with DPPH<sup>•</sup> requires the detailed study of its kinetics as well as geometry and electronic structure of the reactants, intermediates, and products of the reaction in different media using quantum-chemical methods. Such studies have been performed for synthetic sterically hindered phenols [2].

This study aimed to investigate the mechanisms of the reaction of natural di- and trihydroxybenzenes with DPPH<sup>•</sup> in aprotic solvents differing in the polarity, using experimental and quantum-chemical methods.

The following di- and trihydroxybenzenes and their derivatives (**1–8**) belonging to simple plant phenols were studied (Scheme 2).

To study the effect of the medium polarity on the reaction of phenols with DPPH<sup>•</sup> the following non-ionizing solvents were chosen: benzene, dimethylsulfoxide, and their mixtures in different ratios.

## Scheme 1.



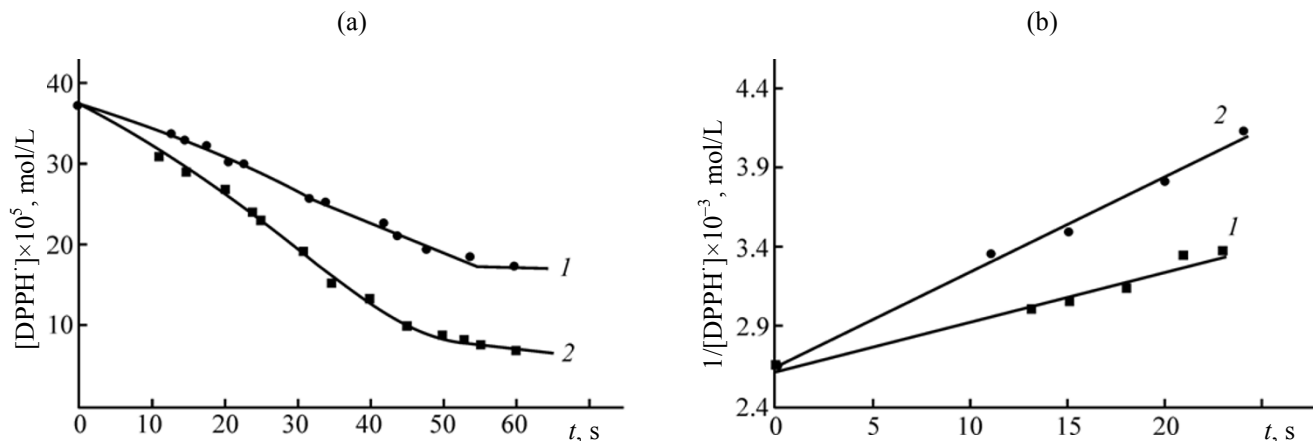


**Fig. 1.** Kinetic curves of DPPH' consumption in the reaction with hydroxybenzenes in benzene at  $293 \pm 2$  K (a) and the same curves plotted in the second-order coordinates (b): (1) pyrocatechol ( $c = 3.77 \times 10^{-4}$  mol/L) and (2) pyrogallol ( $c = 3.79 \times 10^{-4}$  mol/L).

**Reactions in aprotic nonpolar solvent.** Figure 1a displays the kinetic curves of DPPH' concentration change in the reaction with di- and trihydroxybenzenes in a nonpolar non-ionizing solvent—benzene. Determination of the stoichiometry parameters of the reaction revealed that the starting parts of the kinetic curves follow the second-order reaction kinetics (Fig. 1b). The pseudo first orders with respect to the radical and the phenol were found if the other component was taken in a huge excess (10–15 times) with respect to the concerned species. The reaction rate orders were independent of the phenol structure. The kinetic equation for the reaction rate ( $v$ ) could be written as follows (1).

$$v = k_{\text{benz}} [\text{DPPH}'] [\text{PhOH}]. \quad (1)$$

The rate constants ( $k_{\text{benz}}$ ) values as the parameter of the antiradical activity are collected in Table 1; the data showed that the compounds containing hydroxyl groups in the *meta* positions (2, 3, and 7) practically did not react with DPPH'. *Para*- and *ortho*-

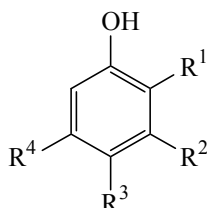
hydroxybenzenes 4–6 and 8 were the most active in that reaction.

The rate constants of the reaction of DPPH' with phenols were determined at different temperatures and processed using the Arrhenius (Fig. 2a) and Eyring (Fig. 2b) equations; that gave the corresponding activation parameters of the reaction: activation energy ( $E_a$ ), preexponent factor ( $A$ ), and activation enthalpy ( $\Delta H^\ddagger$ ). The  $E_a$  ranged between 10 and 40 kJ/mol, typical of the reactions involving radicals (Table 1).

In the studied reaction, the hydrazyl radical was deactivated by phenolic compounds to form stable diphenylpicrylhydrazine (DPPH–H) and inactive phenoxyl radical (PhO) (Scheme 3).

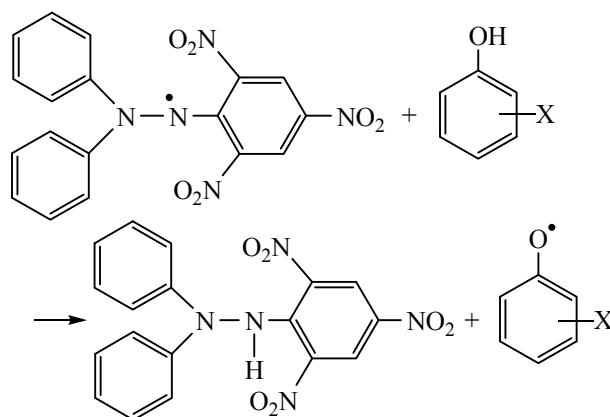
The reaction proceeds in a single stage in nonpolar medium and can occur as simultaneous transfer of electron and proton to the radical (known as the Hydrogen Atom Transfer mechanism, HAT) or as

**Scheme 2.**



$R^1 = \text{OH}$ ,  $R^2 = R^3 = R^4 = \text{H}$  (1);  $R^1 = R^3 = R^4 = \text{H}$ ,  $R^2 = \text{OH}$  (2);  $R^1 = R^3 = \text{H}$ ,  $R^2 = \text{OH}$ ,  $R^4 = \text{CH}_3$  (3);  $R^1 = R^2 = R^4 = \text{H}$ ,  $R^3 = \text{OH}$  (4);  $R^1 = R^2 = R^4 = \text{H}$ ,  $R^3 = \text{OCH}_3$  (5);  $R^1 = R^2 = \text{OH}$ ,  $R^3 = R^4 = \text{H}$  (6);  $R^1 = R^3 = \text{H}$ ,  $R^2 = R^4 = \text{OH}$  (7);  $R^1 = R^3 = \text{OH}$ ,  $R^2 = R^4 = \text{H}$  (8).

**Scheme 3.**



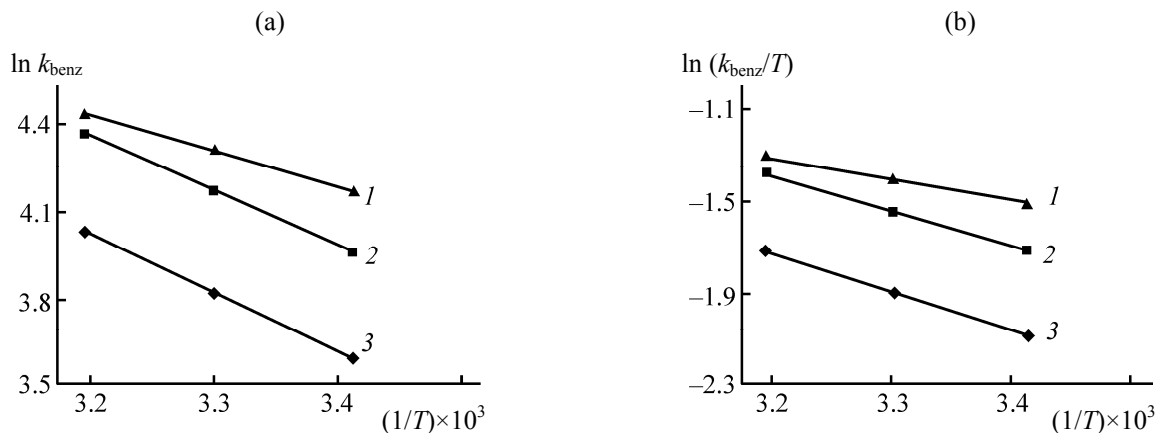


**Fig. 2.** Determination of activation parameters of the reaction between DPPH<sup>•</sup> radical with pyrogallol (1), hydroquinone (2), and pyrocatechol (3) in benzene using the Arrhenius (a) and Eyring (b) equations.

coupled process initiated by electron transfer from the antioxidant molecule to the radical center, followed by proton transfer to the formed electron pair (Proton-Coupled Electron Transfer, PCET) [2]. Since in both cases the rate-limiting step involved electron and proton, deuterium isotope effect should be operative for these mechanisms.

To study the deuterium isotope effect, we prepared the deuterium derivative of phenol (PhOD) via the isotope exchange between hydroxybenzene and deuterium dioxide (D<sub>2</sub>O) in DMSO. NMR spectroscopy monitoring revealed that the phenols were transformed into the corresponding deuterated derivatives within 25–30 min (conversion 97–98%), as confirmed by practically complete vanishing of the <sup>1</sup>H NMR signals of the O–H protons at 9.4–12.4 ppm.

Rate constant of the DPPH<sup>•</sup> reaction with phenols in the presence of hydroxybenzene ( $k_{\text{PhOH}}$ ) was higher

than that in the presence of deuterated PhOD ( $k_{\text{PhOD}}$ ) (Fig. 3). The presence of the pronounced deuterium isotope effect ( $k_{\text{PhOH}}/k_{\text{PhOD}}$ ) (Table 1) confirmed the transfer of proton in the reaction (Scheme 2) and, hence, the possibility of the DPPH<sup>•</sup> reaction with PhOH via HAT as well as PCET mechanism.

Since the mentioned mechanisms are single-stage and result in the formation of identical products, it is impossible to experimentally distinguish between them, and solid confirmation of the mechanism requires detailed study of the structure of the transition state that will be further conducted by quantum-chemical methods. At the current stage, we suggest that the proton transfer can occur via either HAT or PCET mechanism.

To confirm the reaction (Scheme 2) occurrence via the HAT/PCET mechanism, we supplemented the deuterium isotope effect experiment with the simulation of

**Table 1.** Experimental values of kinetic and activation parameters of di- and trihydroxybenzenes with DPPH in benzene at 293 K

Comp. no.	$k_{\text{benz}}$ , L mol <sup>-1</sup> s <sup>-1</sup>	$E_a$ , kJ/mol	$A$	$\Delta H^\ddagger$ , kJ/mol	$k_{\text{PhOH}}/k_{\text{PhOD}}$
1	36.2±1.4	17±1	(3.89±0.21)×10 <sup>4</sup>	14±1	2.5
2	(3.07±0.14)×10 <sup>-3a</sup>	38±2	(5.36±0.26)×10 <sup>3</sup>	36±2	3.1 <sup>a</sup>
3	(1.83±0.07)×10 <sup>-3a</sup>	40±2	(6.8±0.3)×10 <sup>3</sup>	38±2	3.3 <sup>a</sup>
4	52.6±2.1	15±1	(2.48±0.14)×10 <sup>4</sup>	13±1	2.6
5	60.3±2.2	12±1	(8.3±0.3)×10 <sup>3</sup>	10±1	2.4
6	65.2±2.2	10±1	(3.95±0.21)×10 <sup>3</sup>	8±1	2.2
7	(1.12±0.05)×10 <sup>-3a</sup>	41±2	(6.1±0.3)×10 <sup>3</sup>	39±2	3.1 <sup>a</sup>
8	60.4±2.2	12±2	(8.3±0.3)×10 <sup>3</sup>	10±1	2.4

<sup>a</sup> For *meta*-hydroxybenzenes slowly reacting with DPPH in benzene, the  $k_{\text{benz}}$  and  $k_{\text{PhOH}}/k_{\text{PhOD}}$  values at 318 K are given.

geometry, electronic, and thermochemical parameters of the reactants, intermediates, and products of the reaction between DPPH and phenols **1–8** by means of the density functional theory (DFT) using the B3LYP hybrid functional [6, 7] (Gaussian 09 [8]). The choice of B3LYP was supported by the available report [9] on successful use of that functional for a series of compounds of phenol type. Preliminary search for major conformers was performed using the PM6 semiempirical method [10]. The structures with the lowest electronic energy were used as the starting approximation for the non-empirical simulation at the B3LYP/6-311++G(d,p) level (including polarization and diffuse functions for all the atoms) for the closed-shell structures and the UB3LYP/6-311++G(d,p) level for the open-shell systems. In the latter case, the expected values of the operator of the squared full spin moment  $\langle S^2 \rangle$  were checked: before the application of the operator of elimination of the first admixture spin state, the  $\langle S^2 \rangle$  values were 0.76–0.78, being exactly 0.75 after its application; that corresponded to the ideal value for the purely doublet state and evidenced the marginal contribution of the states with higher multiplicity into the wave function [11].

Geometry of the structures was optimized over all independent variables without any symmetry restrictions. The obtained results correspond to the ground state under standard conditions ( $T = 298$  K,  $P = 1$  atm). The simulation was initially run in the gas phase, and then the output was used as the starting point for the complete optimization of the structure accounting for the solvent (benzene or DMSO) using the polarizable continuum medium PCM approach [12]. To construct the cavity of the solute, atomic radii from the UFF force field model were set [13]. We performed harmonic vibrational analysis for the equilibrium structures, in order to testify the correspondence to the minimum and to calculate their thermochemical parameters. The vibration frequencies were not scaled.

Basing on the obtained data, we determined thermodynamic parameters of the reaction (Scheme 2) in different media [the changes of enthalpy ( $\Delta_r H^{\text{HAT/PCET}}$ ) and Gibbs free energy ( $\Delta_r G^{\text{HAT/PCET}}$ )] (Table 2) using Eqs. (2), (3).

$$\Delta_r H^{\text{HAT/PCET}} = (H_{\text{DPPH-H}} + H_{\text{PhO}^\cdot}) - (H_{\text{DPPH}^\cdot} + H_{\text{PhOH}}), \quad (2)$$

$$\Delta_r G^{\text{HAT/PCET}} = (G_{\text{DPPH-H}} + G_{\text{PhO}^\cdot}) - (G_{\text{DPPH}^\cdot} + G_{\text{PhOH}}), \quad (3)$$

with  $H_{\text{DPPH-H}}$ ,  $G_{\text{DPPH-H}}$ ,  $H_{\text{PhO}^\cdot}$ ,  $G_{\text{PhO}^\cdot}$ ,  $H_{\text{DPPH}^\cdot}$ ,  $G_{\text{DPPH}^\cdot}$ ,  $H_{\text{PhOH}}$ , and  $G_{\text{PhOH}}$  being enthalpies ( $H$ ) and Gibbs free energies ( $G$ ) of the DPPH-H molecule, phenoxyl radical, DPPH $^\cdot$  radical, and PhOH molecule, respectively.

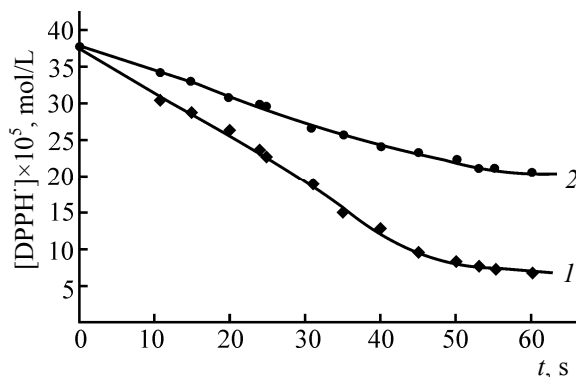


**Fig. 3.** Kinetic curves of DPPH $^\cdot$  consumption in the reaction with pyrogallol (1) ( $c = 3.79 \times 10^{-4}$  mol/L) and its deuterated derivative (2) ( $c = 3.79 \times 10^{-4}$  mol/L) in benzene at  $293 \pm 2$  K.

Energy of homolytic cleavage, i.e. the strength of the O–H bond ( $D_{\text{O-H}}$ ) in a hydroxybenzene molecule was calculated using Eq. (4).

$$D_{\text{O-H}} = (H_{\text{H}} + H_{\text{PhO}^\cdot}) - H_{\text{PhOH}}, \quad (4)$$

with  $H_{\text{H}}$ , enthalpy of hydrogen atom [simulated values  $-1312.479574$  kJ/mol (gas),  $-1312.518956$  kJ/mol (benzene), and  $-1312.547837$  kJ/mol (DMSO)].

Analysis of thermodynamic parameters obtained for the solvents medium revealed that the reaction (Scheme 2) showed that the reaction was more exothermic in benzene than in DMSO. The highest  $\Delta_r H^{\text{HAT/PCET}}$  values were found for trihydroxybenzenes **6** and **8** exhibiting the highest antiradical activity in the reaction with DPPH $^\cdot$ . The same was found for the Gibbs energy of the reaction. The increase in the medium polarity led to the increase in the  $\Delta_r G^{\text{HAT/PCET}}$  value, hence, the reaction of PhOH with DPPH $^\cdot$  via the HAT/PCET mechanism was more thermodynamically favorable in benzene.

Since the lowest  $D_{\text{O-H}}$  value for the hydroxybenzene molecule determined the HAT/PCET (Table 2), it was logical to assume the correlation between  $D_{\text{O-H}}$  and the substance reactivity ( $\ln k_{\text{benz}}$ ). For example, it was shown that the experimental rate constant in benzene medium decreased with the increase in the  $D_{\text{O-H}}$  value (Fig. 4a).

$$\ln k_{\text{benz}} = (11.0 \pm 0.7) - (21.8 \pm 2.1) \times 10^{-3} D_{\text{O-H}(\text{benz})},$$

$$n = 5, r = 0.986, r^2 = 0.972, F = 106, p < 0.002.$$

with  $n$ , number of the experiments;  $r$ , correlation coefficient;  $r^2$ , determination coefficient;  $F$ , the Fischer's parameter;  $p$ , significance level.

**Table 2.** Enthalpy change ( $\Delta_r H$ , kJ/mol) and Gibbs free energy change ( $\Delta_r G$ , kJ/mol) of the studied reactions, ionization potential ( $PI$ , kJ/mol), and strength of the weakest O–H bond ( $D_{O-H}$ , kJ/mol) of hydroxybenzenes **1–8** in different media simulated using the B3LYP/6-311++G(d,p) method

Comp. no.	Gas			Benzene			DMSO		
	$D_{O-H(gas)}$	$\Delta_r H^{HAT/PCET}$	$\Delta_r G^{HAT/PCET}$	$D_{O-H(benz)}$	$\Delta_r H^{HAT/PCET}$	$\Delta_r G^{HAT/PCET}$	$D_{O-H(DMSO)}$	$\Delta_r H^{HAT/PCET}$	$\Delta_r G^{HAT/PCET}$
HAT/PCET mechanism (Scheme 2)									
<b>1</b>	347	–55.0	–11.4	340	–42.4	–3.2	331	–25.3	–10.2
<b>2</b>	345	–56.3	–13.5	343	–38.8	–0.2	342	–13.8	24.6
<b>3</b>	351	–51.2	–9.3	347	–35.2	2.7	343	–12.8	25.2
<b>4</b>	326	–75.9	–34.9	322	–60.1	–20.6	318	–37.8	1.3
<b>5</b>	353	–77.8	–34.7	320	–62.2	–23.1	316	–40.0	–1.1
<b>6</b>	315	–138.4	–40.9	312	–95.6	–29.2	307	–72.0	98.2
<b>7</b>	351	–77.1	–8.7	348	–34.2	3.9	345	–10.7	27.4
<b>8</b>	320	–81.8	–37.2	317	–64.9	–24.4	311	–64.9	–2.8
Comp. no.	$PI_{gas}$	$\Delta_r H^{ET-PT}$	$\Delta_r G^{ET-PT}$	$PI_{benz}$	$\Delta_r H^{ET-PT}$	$\Delta_r G^{ET-PT}$	$PI_{DMSO}$	$\Delta_r H^{ET-PT}$	$\Delta_r G^{ET-PT}$
ET–PT mechanism (Scheme 3)									
<b>1</b>	769	440	127	659	256	22.2	565	–94	–33.5
<b>2</b>	779	450	136	669	242	31.5	588	–84	–23.6
<b>3</b>	768	438	58.6	659	256	20.8	584	–88	–35.9
<b>4</b>	746	417	8.7	636	233	–17.3	556	–116	–55.6
<b>5</b>	725	396	140	662	218	–17.6	547	–59	–65.3
<b>6</b>	737	382	121	655	227	18.7	536	–119	–34.4
<b>7</b>	778	423	135	670	267	32.8	591	–81	–21.2
<b>8</b>	726	398	85.8	620	217	–15.1	543	–129	–67.1

**Table 3.** Experimental values of the rate constant ( $k_{DMSO-benz}$ ) of hydroxybenzenes reaction with DPPH $\cdot$  at different fractions of DMSO (vol %) in its mixture with benzene at 293 $\pm$ 2 K

Comp. no.	$k_{DMSO-benz}$ , L mol $^{-1}$ s $^{-1}$				$k_{DMSO}/k_{benz}$	$k_{PhOH}/k_{PhOD}$
	0	30	70	100		
<b>1</b>	36.1 $\pm$ 1.4	(1.58 $\pm$ 0.12) $\times 10^2$	(3.10 $\pm$ 0.18) $\times 10^2$	(3.7 $\pm$ 0.3) $\times 10^2$	10.2	0.98
<b>4</b>	52.6 $\pm$ 2.1	(1.91 $\pm$ 0.12) $\times 10^2$	(4.02 $\pm$ 0.18) $\times 10^2$	(5.5 $\pm$ 0.3) $\times 10^2$	10.5	0.96
<b>5</b>	60.3 $\pm$ 2.2	(2.51 $\pm$ 0.15) $\times 10^2$	(5.4 $\pm$ 0.3) $\times 10^2$	(6.2 $\pm$ 0.3) $\times 10^2$	10.3	1.02
<b>6</b>	65.2 $\pm$ 2.2	(3.56 $\pm$ 0.18) $\times 10^2$	(7.9 $\pm$ 0.4) $\times 10^2$	(9.8 $\pm$ 0.4) $\times 10^2$	15.0	0.98
<b>8</b>	60.4 $\pm$ 2.2	(3.11 $\pm$ 0.18) $\times 10^2$	(6.8 $\pm$ 0.3) $\times 10^2$	(7.3 $\pm$ 0.4) $\times 10^2$	12.1	1.01

It was noted that for hydroxybenzenes with OH groups in the *meta* positions (compounds **2**, **3**, and **7**), the strength of the O–H bonds were the highest of the studied phenols, in agreement with their low reactivity in the reaction with the hydrazyl radical.

In summary, the data on deuterium isotopic effect, the results of quantum-chemical simulation of thermodynamic parameters of the reaction, and regression analysis of the structure–reactivity relationship led to a conclusion that the reaction of the DPPH $\cdot$  radical with

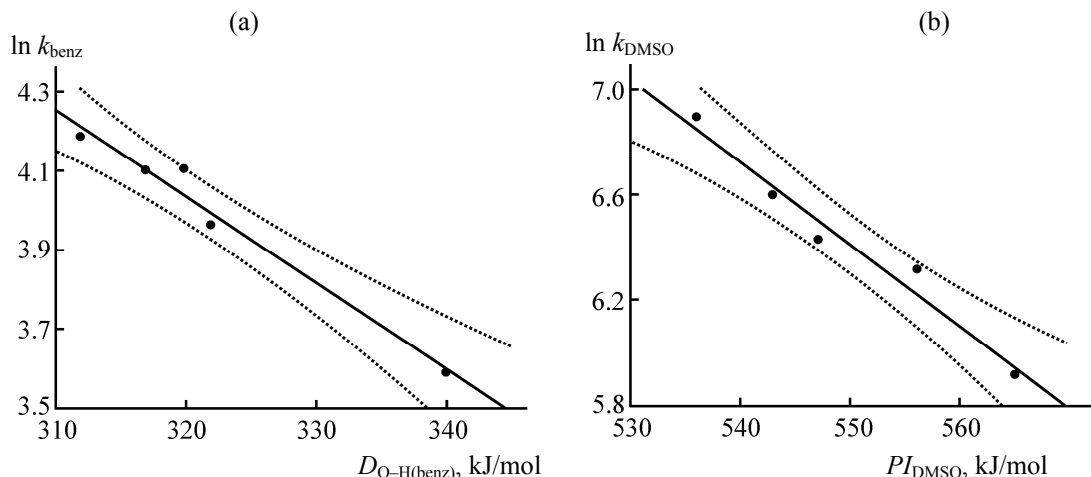


Fig. 4. Correlation of hydroxybenzenes reactivity with the structural parameters in benzene (a) and DMSO (b).

non-hindered di- and trihydroxybenzenes and their derivatives in aprotic nonpolar media occurred via the HAT/PCET hydrogen transfer mechanism.

**Reactions in aprotic polar solvent.** The addition of DMSO to the studied system resulted in sharp increase in reactivity of the hydroxybenzenes with respect to DPPH $\cdot$  (Table 3). That could be related to the effect of specific solvation (formation of hydrogen bonds between the radical and the solvent molecules) as well as to nonspecific solvation (the increase in the dielectric permittivity of the medium  $\epsilon$ ).

The derived linear behavior in the coordinates of the Leidler–Eyring equation [14] showed that the rate of the studied reaction in the binary solvent was strongly dependent on the dielectric constant of the medium (Fig. 5).

$$\log k_{\text{DMSO-benz}} = \lg k_0 - 2.3/RT(\mu_{\text{PhOH}}^2/r_{\text{PhOH}}^2 + \mu_{\text{DPPH}\cdot}^2/r_{\text{DPPH}\cdot}^2 - \mu_{\neq}^2/r_{\neq}^2) \cdot [(\epsilon - 1)/(2\epsilon + 1)]. \quad (5)$$

Here,  $k_{\text{DMSO-benz}}$  is the reaction rate constant in the mixed solvent;  $k_0$  is the reaction rate constant in gas phase with  $\epsilon = 1$ ;  $\epsilon$  is dielectric constant of the mixed solvent;  $2.3/RT(\mu_{\text{PhOH}}^2/r_{\text{PhOH}}^2 + \mu_{\text{DPPH}\cdot}^2/r_{\text{DPPH}\cdot}^2 - \mu_{\neq}^2/r_{\neq}^2)$  is the value reflecting the effect of the solvent on the reaction rate constant;  $\mu_{\neq}$ ,  $\mu_{\text{PhOH}}$ , and  $\mu_{\text{DPPH}\cdot}$  are dipole moments and  $r_{\neq}$ ,  $r_{\text{PhOH}}$ , and  $r_{\text{DPPH}\cdot}$  are the radii of the active complex, the phenol, and the hydrazyl radical, respectively;  $(\epsilon - 1)/(2\epsilon + 1)$  (the Kirkwood function) determines the solvent polarity.

The increase in the reaction rate with the increase in the mixed solvent polarity followed the linear proportionality, and the slope  $2.3/RT(\mu_{\text{PhOH}}^2/r_{\text{PhOH}}^2 + \mu_{\text{DPPH}\cdot}^2/r_{\text{DPPH}\cdot}^2 - \mu_{\neq}^2/r_{\neq}^2)$

of the linear regression (5) was positive (Fig. 5). That pointed that the transition complex was more polar and better solvated than the starting reagents, and the reaction was accelerated. In view of that, it could be assumed that the increase in the medium dielectric constant (that could change the reaction mechanism) rather than specific solvation had the predominant effect on the radical activity of hydroxybenzenes in polar media with poor ionizing ability.

The so high sensitivity of the reaction rate to the medium polarity is typical of the reactions with electron transfer as the limiting stage, as confirmed by the absence of the deuterium isotopic effect (the

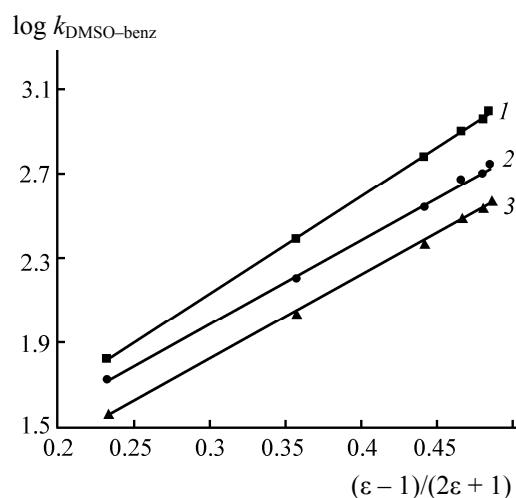
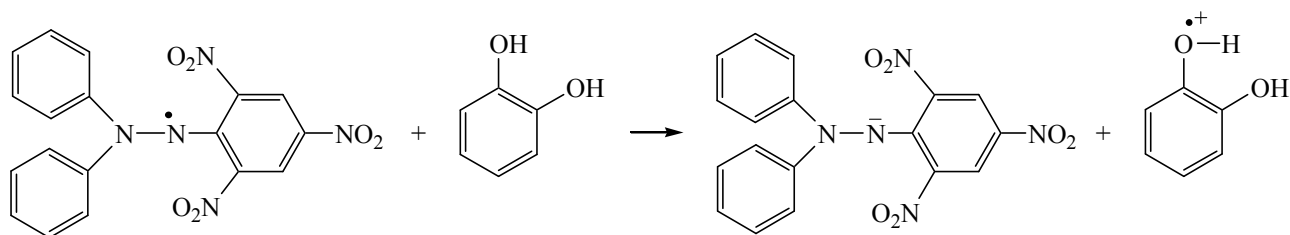
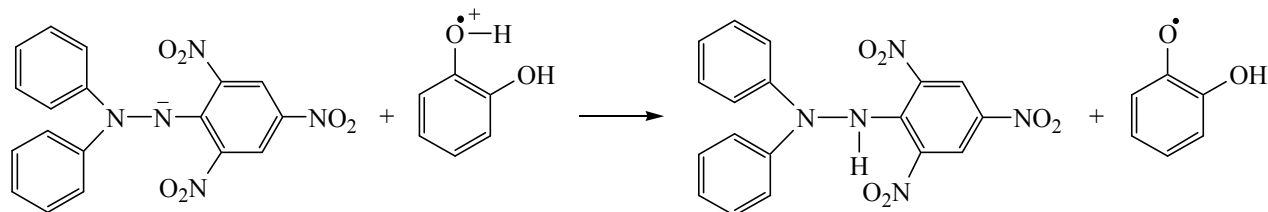


Fig. 5. The Leidler–Eyring plots for the reaction of DPPH $\cdot$  radicals with hydroxybenzenes in a benzene–DMSO mixture: (1) pyrogallol, (2) hydroquinone, and (3) pyrocatechol.

Scheme 4.



Scheme 5.



$k_{\text{PhOH}}/k_{\text{PhOD}}$  ratio was close to unity) in DMSO medium (Table 3), in contrast to benzene.

In the case of polar aprotic solvent, the interaction of the hydrazyl radical with the studied phenols could be represented as successive transfer of electron (slow, Scheme 4) to form the phenol cation-radical as the intermediate, followed by proton transfer (fast, Scheme 4) (ET–PT).

Likely, the increase in the medium dielectric constant led to significant charge separation in the transition state (Scheme 5) and favored the subsequent decomposition of the active complex with charge transfer into the ions.

Thermodynamic parameters of the rate-limiting stage (Scheme 3) in different media were calculated using Eqs. (6), (7).

$$\Delta_r H^{\text{ET-PT}} = (H_{\text{DPPH}^-} + H_{\text{PhO}^+\cdot\text{H}}) - (H_{\text{DPPH}\cdot} + H_{\text{PhOH}}), \quad (6)$$

$$\Delta_r G^{\text{ET-PT}} = (G_{\text{DPPH}^-} + G_{\text{PhO}^+\cdot\text{H}}) - (G_{\text{DPPH}\cdot} + G_{\text{PhOH}}). \quad (7)$$

with  $H_{\text{DPPH}^-}$ ,  $G_{\text{DPPH}^-}$ ,  $H_{\text{PhO}^+\cdot\text{H}}$ , and  $G_{\text{PhO}^+\cdot\text{H}}$  being enthalpy ( $H$ ) and Gibbs free energy ( $G$ ) of the DPPH anion and the PhOH cation-radical, respectively.

Analysis of the calculated enthalpies and Gibbs free energies showed that the ET–PT mechanism of electron transfer was thermodynamically more favorable in DMSO than in benzene (Table 2).

The parameter related to the occurrence of the ET–PT mechanism is the enthalpy of electron transfer from the antioxidant, i.e. its ionization potential ( $PI$ ). Table 2

lists the calculated adiabatic ionization potentials of the hydroxybenzenes.

$$PI = H_{\text{PhO}^+\cdot\text{H}} - H_{\text{PhOH}}.$$

The  $PI$  values were notably reduced when the solvent became more polar. It was remarkable that  $\ln k_{\text{DMSO}}$  was better related to  $PI_{\text{DMSO}}$  than to the bond strength O–H of the hydroxybenzenes.

$$\ln k_{\text{DMSO}} = (23.6 \pm 1.8) - (3.1 \pm 0.3) \times 10^{-2} PI_{\text{DMSO}},$$

$$n = 5, r = 0.984, r^2 = 0.968, F = 89.6, p < 0.002.$$

The increase in ionization potential of hydroxybenzenes resulted in the regular decrease in their reactivity (Fig. 4b), possibly related to deceleration of electron transfer from phenol to the radical in the frames of the ET–PT mechanism.

Comparison of antiradical activity of hydroxybenzenes in the reaction with the hydrazyl radical showed that as benzene was changed to DMSO, the ET–PT mechanism became dominant over the HAT/PCET one, accelerating the process ( $k_{\text{DMSO}}/k_{\text{benz}}$ ) by 10–15 times (Table 3).

In summary, the elucidated mechanism of antiradical activity of di- and trihydroxybenzenes as structural elements of more complex natural phenols suggested that the similar processes could underlie the action of other classes of compounds (phenolcarboxylic and hydroxycinnamic acids, flavonoids and their glycosides, etc.); that would require further experimental confirmation. The suggested possible mechanism of the reaction between a DPPH stable

radical with molecular forms of phenols allows simulation of their behavior in organic substrates (oils, fats, and lipids), aqueous, and aqueous-organic biological systems with low pH, suppressing dissociation of phenolic compounds.

### EXPERIMENTAL

The DPPH stable radical and DMSO (Sigma Aldrich) were used. The radical solvent in aprotic solvents was violet, the absorbance maximum being 520 nm. Storage of DPPH in DMSO and benzene in dark during 72 h did not affect the solution absorbance in its maximum. DMSO was purified via the conventional procedure [15]. Hydroxybenzenes (chemical pure grade) were purified via repeated recrystallization from ethanol and dried at 40°C under nitrogen, followed by sublimation in vacuum. Oxyhydroquinone was synthesized as described elsewhere [16].

The experiments were performed at 293–318 K and starting concentrations of the reactants  $10^{-4}$ – $10^{-5}$  mol/L. A phenol solution was mixed with DPPH solution (the reactants were taken in equimolar concentration), and the absorbance was measured using an SF-2000 spectrophotometer (Russia). DPPH concentration was calculated using the molar absorptivity values  $\varepsilon_{\text{DMSO}} = 1.2 \times 10^4 \text{ L mol}^{-1} \text{ cm}^{-1}$  and  $\varepsilon_{\text{benz}} = 8.77 \times 10^3 \text{ L mol}^{-1} \text{ cm}^{-1}$ .

$^1\text{H}$  NMR spectra were recorded using a Bruker Avance-II-400 spectrophotometer (Germany) with working frequency 400 MHz. Spectra of hydroxybenzenes in DMSO- $d_6$  and in the DMSO- $d_6$ - $\text{D}_2\text{O}$  mixtures (with  $\text{D}_2\text{O}$  volume fraction 20 to 30%) were recorded at 298 K ( $c_{\text{PhOH}} = 0.025 \text{ mol/L}$ ).

### REFERENCES

- Vermerris, W. and Nicolson, R., *Phenolic Compound Biochemistry*, Dodrecht: Springer, 2006.
- Foti, M.C., Daquino, C., Mackie, I.D., DiLabio, G.A., and Ingold, K.U., *J. Org. Chem.*, 2008, vol. 73, p. 9270. doi 10.1021/jo8016555
- Litwinienko, G. and Ingold, K.U., *J. Org. Chem.*, 2005, vol. 70, no. 68, p. 8982. doi 10.1021/jo051474p
- Sun, B., Spranger, I., Yang, J., Leandro, C., Guo, L., Canrio, S., Zhao, Y., and Wu, C., *J. Agric. Food Chem.*, 2009, vol. 57, no. 18, p. 8623. doi 10.1021/jf901610h
- Shang, Y.-J., Liu, B.-Y., and Zhao, M.-M., *Czech J. Food Sci.*, 2015, vol. 33, p. 210. doi 10.17221/611/2014-CJFS
- Frisch, M.J., Trucks, G.W., Schlegel, H.B., Scuseria, G.E., Robb, M.A., Cheeseman, J.R., Scalmani, G., Barone, V., Mennucci, B., Petersson, G.A., Nakatsuji, H., Caricato, M., Li, X., Hratchian, H.P., Izmaylov, A.F., Bloino, J., Zheng, G., Sonnenberg, J.L., Hada, M., Ehara, M., Toyota, K., Fukuda, R., Hasegawa, J., Ishida, M., Nakajima, T., Honda, Y., Kitao, O., Nakai, H., Vreven, T., Montgomery, J.A., Jr., Peralta, J.E., Ogliaro, F., Bearpark, M., Heyd, J.J., Brothers, E., Kudin, K.N., Staroverov, V.N., Keith, T., Kobayashi, R., Normand, J., Raghavachari, K., Rendell, A., Burant, J.C., Iyengar, S.S., Tomasi, J., Cossi, M., Rega, N., Millam, J.M., Klene, M., Knox, J.E., Cross, J.B., Bakken, V., Adamo, C., Jaramillo, J., Gomperts, R., Stratmann, R.E., Yazyev, O., Austin, A.J., Cammi, R., Pomelli, C., Ochterski, J.W., Martin, R.L., Morokuma, K., Zakrzewski, V.G., Voth, G.A., Salvador, P., Dannenberg, J.J., Dapprich, S., Daniels, A.D., Farkas, O., Foresman, J.B., Ortiz, J.V., Cioslowski, J., and Fox, D.J., *Gaussian 09*, Revision B.01 Gaussian, Inc., Wallingford CT, 2010.
- Becke, A.D., *J. Chem. Phys.*, 1993, vol. 98, p. 5648. doi 10.1063/1.464913
- Lee, C., Yang, W., and Parr, R.G., *Phys. Rev. (B)*, 1988, vol. 37, p. 785. doi 10.1103/PhysRevB.37.785
- Weinberg, D.R., Gagliardi, C.J., Hull, J.F., Murphy, C.F., Kent, C.A., Westlake, B., Paul, A., Ess, D.H., McCafferty, G.D., and Meyer, T.J., *Chem. Rev.*, 2007, vol. 107, no. 11, p. 5004. doi 10.1021/cr0500030
- Stewart, J.J.P., *J. Mol. Model.*, 2007, vol. 13, p. 1173.
- Young, D., *Computational Chemistry: A Practical Guide for Applying Techniques to Real World Problems*, New York: Wiley, 2001, p. 227.
- Tomasi, J., Mennucci, B., and Cammi, R., *Chem. Rev.*, 2005, vol. 105, p. 2999. doi 10.1021/cr9904009.
- Rappe, A.K., Casewit, C.J., Colwell, K.S., Goddard, W.A., and Skiff, W.M., *J. Am. Chem. Soc.*, 1992, vol. 114, p. 10024. doi 10.1021/ja00051a040.
- Denisov, E.T., *Kinetika gomogennykh khimicheskikh reaktsii* (Kinetics of Homogeneous Chemical Reactions), Moscow: Vysshaya Shkola, 1978, p. 100.
- Armarego, W.L.F. and Chai, C.L.L., *Purification of Laboratory Chemicals*, Burlington: Elsevier Science, 2003.
- Preparative Organic Chemistry*, Wolfson, N.S., Ed., Moscow: Gos. Khim. Izd., 1959.